2nd Symposium on New Trends in Nuclear and Medical Physics, Poland, September 24–26, 2025

Two-Exponential Decay of Acridine Orange

F. Giacosa[a,b,*], A. Kolbus[a], K. Kyziol[a], M. Plodowska[a], M. Piotrowska[a], K. Szary[a] and A. Vereijken[a]

[a] *Jan Kochanowski University, ul. Żeromskiego 5, 25-369 Kielce, Poland*
[b] *Goethe University, Theodor-W.-Adorno-Platz 1, 60323 Frankfürt am Main, Germany*

Doi: 10.12693/APhysPolA.148.S110 *e-mail: fgiacosa@ujk.edu.pl

In this work, we experimentally study the fluorescence decay of acridine orange at late times to test whether late-time power-law behaviour emerges — a feature expected to be very small but consistent with quantum mechanical and quantum field theoretical predictions. Using two distinct photon detectors, we find that the data are well described by the sum of two exponential functions with lifetimes $\tau_1 = 1.7331 \pm 0.001$ ns and $\tau_2 = 5.948 \pm 0.012$ ns, in agreement with values reported in the literature. Although no deviation from the exponential decay law is observed, this study serves as a reliable test of the experimental setup and enables a precise determination of the sample lifetimes.

topics: quantum mechanics (QM), fluorescence, time-correlated single photon counting spectroscopy, lifetime

1. Introduction

The standard radioactive decay law describes the change in the number of elements in a sample as $N(t) = N_0 \mathrm{e}^{-t/\tau}$ — an exponential function. However, this successful phenomenological formulation is not strictly reproduced within the framework of quantum mechanics (QM) and quantum field theory (QFT), according to which $N(t) = N_0\, P(t)$, where $P(t)$ is the survival probability as a function of time t of a single unstable quantum state. The quantity $P(t)$ emerges as the modulus squared of the Fourier transform of the energy distribution $\rho(E)$ of the unstable quantum state/particle, e.g. [1],

$$P(t) = \left| \int_{E_{th}}^{\infty} \mathrm{d}E\ \rho(E) \mathrm{e}^{-\mathrm{i}Et/\hbar} \right|^2, \tag{1}$$

where E_{th} is the lowest admissible energy. Only in the limit $E_{th} \to -\infty$ and for a Breit–Wigner distribution $\rho(E)$, the decay is purely exponential. If, instead, the expectation value of the Hamiltonian operator H is finite, then $P'(0) = 0$. If also the H^2-expectation value is finite, $P(t)$ can be approximated at short times as $P(t) \simeq 1 - t^2/t_Z^2$ with $\tau_Z = \hbar/\sigma_E$, where σ_E is the standard deviation of the energy distribution. This deviation from the exponential decay law at short times is linked to the quantum Zeno effect (QZE), i.e., freezing in its initial state if probed sufficiently often [2–6]. On the other hand, at large times the survival probability $P(t)$ is well described by a power law, $P(t) \sim t^{-(\beta-1)}$, leading to the decay rate intensity $I(t) \sim t^{-\beta}$. This is a direct consequence of the presence of the energy threshold E_{th} [7]. Both mentioned effects are predicted in the framework of QM [1, 8, 9] and also QFT [10–13] and emerge from their very first principles. However, the deviations are typically very small in the case of elementary systems/transitions. As the 'parade' example of the $2P$–$1S$ transition of the H-atom shows, short-time deviations take place at time $10^{-8}\tau$ and late-time deviations at time $\sim 125\tau$ ($\tau = 1.595$ ns). Thus, measurements at very early and very late times are extremely challenging, as the predicted quantum effects are strongly suppressed [14, 15].

At short times, deviations from the exponential decay law were experimentally verified in the study of quantum tunneling of sodium atoms in an optical potential [16, 17]. (For indirect evidence, see the photonic-waveguide array experiment reported in [18]; strongly decaying systems also display deviations from the Breit–Wigner function [11, 19], which in turn imply a non-exponential behaviour — although such deviation cannot be directly measured due to the extremely short time ($\sim 10^{-23}$ s) involved.)

For long times, the well-known work [20] reports a power law intensity $I(t)$ for various chemical compounds decaying via fluorescence [21]. Very recently, a power law was confirmed by our group in the case of erythrosine B upon using two distinct photodetectors [22]. In both cases, dissolved fluorophores were employed; such systems — even if not as simple as 'more elementary quantum states' because of inhomogeneous broadening of the emission spectrum

TABLE I

Model functions used in the analysis; b is the background. Time $t_0 = 2.24$ ns corresponds (for both channels) to the intensity maximum (and is not a fit parameter).

Model	Fluorescence intensity $I(t)$	Fit parameters
Two-exponential	$I(t) = C_1 \exp\left(-\frac{t-t_0}{\tau_1}\right) + C_2 \exp\left(-\frac{t-t_0}{\tau_2}\right) + b$	$\chi^2(C_1, \tau_1, C_2, \tau_2, b)$
Non-exponential	$I(t) = C \exp\left(-\frac{t-t_0}{\tau}\right) + C_p\,(t-t_0)^{-\beta} + b$	$\chi^2(C_0, \tau, C_p, \beta, b)$

caused by the interaction of the compound with the solvent — are thought to still be described by the inherent quantum equation (1).

In this work, we report on the late-time study of a different substance — acridine orange — measured using two photon detectors acting in different ranges. As we shall show, the decay rate can be well described by the sum of two exponential functions, in agreement with a mixture of two quantum states with two distinct lifetimes. The rather precise determination of lifetime(s) is in agreement with values reported in the literature. Moreover, even if no 'quantum' late-time memory effect can be seen, this study provides a valuable test of our experimental approach aimed at investigating the late-time decay law.

2. Basic features of fluorescence

The excited states of fluorophores are typical examples of unstable quantum states. These molecules may absorb a photon, which implies the excitation of an electron to higher energy levels denoted by $S_1, S_2, S_3, \ldots$ This electron then undergoes a series of rapid transitions via a non-radiative process referred to as vibrational relaxation. After a short time ($\sim 10^{-12}$ s), the electron is in the lowest vibrational level of the excited electronic state. Subsequently, it may decay into lower electronic states, usually via internal conversion (IC) — which is also a non-radiative process — or via the radiative fluorescence process, which we detect. This transition usually occurs from the lowest vibrational level of the first excited electronic state (S_1) to one of many vibrational levels of the electronic ground state (S_0). According to the Franck–Condon rule, the most probable transitions are those for which the initial and final electronic wave functions overlap the most. Typically, the dynamics of the fluorescence takes place on a timescale of the order of nanoseconds.

3. Description of the device

In this experiment, the time-correlated single photon counting (TCSPC) setup available at the Institute of Biology, Faculty of Natural Sciences, Jan Kochanowski University in Kielce (Poland) was used. It consists of a PicoQuant Laser Combining Unit (LCU), a Nikon Eclipse Ti-E inverted confocal microscope, a detection system, and a PicoQuant PicoHarp 300 TCSPC module.

LCU is composed of two picosecond laser diodes, i.e., PicoQuant LDH-D-C-440 and PicoQuant LDH-D-C-485, emitting light at wavelengths of 438 nm and 485 nm, respectively, with spectral bandwidth between 2 and 8 nm. However, only the latter one was actually used during the measurements. Laser diodes serve as pulsed excitation sources. They operate at 10 MHz frequency (100 ns interval between pulses), and the full width at half maximum (FWHM) of the pulse is less than 120 ps.

The detection setup is composed of two identical PicoQuant PMA Hybrid 40 detectors. They are separated with the dichroic mirror, and every detector is coupled to an individual bandpass filter, i.e., FF01-520/35 and ET600/50. Thus, two independent detection channels can be distinguished that focus on different parts of the spectrum. Channel 1 detects photons of wavelength ranging from 485 to 555 nm, and channel 2 photons from 550 to 650 nm.

Fluorescent samples are placed on the stage of the Nikon Eclipse Ti-E inverted confocal microscope. Thus, the microscope plays an important role in generating and guiding the excitation and emission beams. In our case, it is equipped with one optical fibre transferring the laser pulse from the LCU to the device, and another one extracting the fluorescence signal towards the detection system. The last important piece is the PicoHarp 300 TCSPC module, which is responsible for timing events, analogue-to-digital conversion of the signal, and, finally, assigning particular events to appropriate time bins of the histogram.

4. Description of the experiment

The choice of acridine orange was motivated by the shape of the absorption spectrum that matches the available excitation wavelengths of the LCU, reasonable quantum yields, and its common use in fluorescence studies, which provided a valuable test of our device.

As the first step, the fluorophore was dissolved in water to a final concentration of 10^{-5} mol/dm^3. After transferring the sample to the confocal

microscope, a single real-time test measurement was performed to locate the maximum signal-to-noise ratio. This initial procedure was followed by three 10-minute measurements, each of them made on a different part of the sample. Geometrical conditions remained similar throughout the process. This allows the obtained fluorescence intensity decay curves to be combined into one final data set for an individual detection channel.

5. Results for acridine orange

In the analysis, the coefficients of the functions describing the decay rate were obtained using the χ^2 approach. The standard deviation was estimated with the Poisson statistics. Thus, for a given rate $I(t)$, χ^2 is

$$\chi^2 = \sum_{n=1}^{N_t} \frac{[I_n - I(t_n)]^2}{I(t_n)}, \tag{2}$$

where N_t is the total number of data points. A single exponential function was tested, but it cannot describe the data. Hence, we employed two models presented in Table I, namely a sum of two exponential functions and a non-exponential late-time power law. In the first model, it is assumed that there are two types of initial excited states which decay exponentially, characterised by different lifetimes (τ_1 and τ_2). The second model encodes a late-time QM-inspired power law.

For completeness, we recall that the fluorescence intensity $I(t)$ and the survival probability $P(t)$ are related, with $P(t)$ given by (1). The relation is as follows

$$I(t) = -\frac{\mathrm{d}N}{\mathrm{d}t} = -N_0\, P'(t). \tag{3}$$

6. Discussions

The values of the fit parameters that minimise χ^2 were found numerically[†], and the results are reported in Table II. The following comments are in order:

- For acridine orange, the two-exponential model works well — see the direct comparison between the data and the fit in Fig. 1. The two-exponential decay of acridine orange has previously been observed in aqueous solutions of sodium dodecyl sulfate (SDS) and was attributed to the formation of the micellar structures arising from interactions between the fluorophore and the detergent — see [23, 24]. Also, the obtained values of both lifetimes are in the specified range (1–2 ns for the main and > 3 ns for the other lifetime). This fact suggests that we observe similar aggregates. Interestingly, deviations from the single exponential decay law were also observed earlier for proflavine, which is an acridine's derivative, bound to DNA [25], and for acridine orange itself [26]. However, in the latter case, this effect was caused mainly by the instrument response, and the authors observed a single-lifetime exponential decay after deconvolution of the signal.
- Following a conservative estimate, we quote the following lifetime determinations (inverse-variance weighted mean):

$$\tau_1 = 1.7331 \pm 0.001 \text{ ns},$$
$$\tau_2 = 5.948 \pm 0.012 \text{ ns}. \tag{4}$$

The lifetimes determined by the different detectors are consistent with each other. For channel 1, the standard deviations are 0.0012 ns for τ_1 and 0.0196 ns for τ_2; for channel 2, they are 0.0021 ns and 0.0156 ns. The errors of the fit parameters were taken as the diagonal elements of the covariance matrix

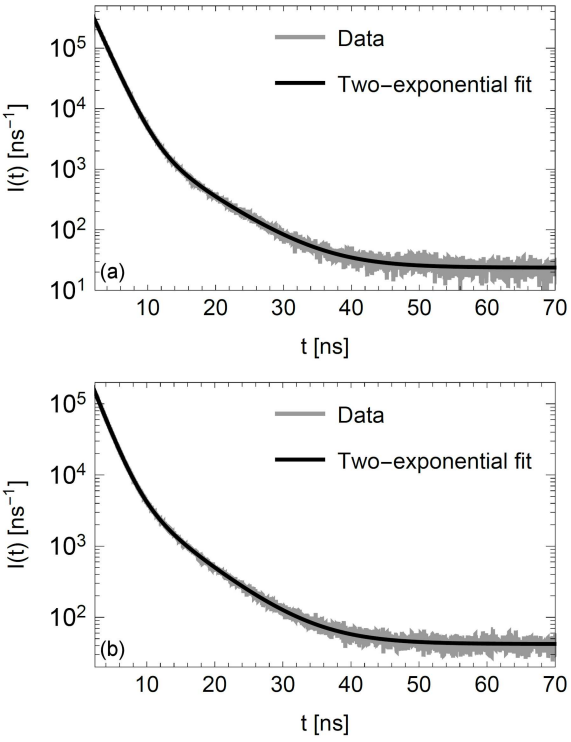

Fig. 1. Fluorescence intensity for both photon detectors ((a) channel 1, (b) channel 2) — comparison between data and two-exponential fitting function.

[†1]Since the excitation is not instantaneous, we start the fit when early-time effects are not relevant. In the case of the non-exponential model, this is also required by the fact that the power function is not a valid approximation in the early-time domain.

TABLE II

Fitting results obtained in the fitting range of 3.200–96.968 ns for acridine orange measurements (Ch. — Channel).

Ch.	χ^2_ν	C_1	τ_1 [ns]	C_2	τ_2 [ns]	b
Two-exponential model						
1	1.0471	278 967	1.7333	6 371.3	5.9459	21.99
2	1.0247	150 898	1.7326	8 983.5	5.9493	42.07
Non-exponential model						
1	11.0881	220 113	1.9360	39 458	1.7386	−1.404
2	14.7270	93 100	2.2649	40 747	2.421	2.421

(the inverse of the Hesse matrix) [27]. As summarized in Table II, the absolute channel-to-channel differences are $|\Delta\tau_1| = 0.0007$ ns and $|\Delta\tau_2| = 0.0034$ ns, both comfortably below the quoted conservative error bars. A noticeable change is observed only in the C_1/C_2 ratio, attributable to the spectral shape and to the position of the spectral window associated with each detection channel.

- The non-exponential model does not offer an acceptable description of the data, see Table II. Thus, no sign of a QM power law is seen in the present data for acridine orange, even if we follow the sample up to more than $10\tau_1$. (Note, the eventual appearance of a power law after about 10 lifetimes [20, 22] implies the existence of an effective threshold E_{th} quite close to the resonance peak [22]. However, the exact nature and emergence of this threshold is not fully understood; thus, at present, one cannot predict the turnover time but can only measure it.)
- In [22], using the same setup, we could measure a power law for erythrosine B. A comparison between that system with the one described in this paper allows us to understand which features favour the detection of the late-time power law. (i) Erythrosine B has a shorter main lifetime ($\tau_1 = 0.45$ ns), thus we could measure the decay curve $I(t)$ for a larger t/τ_1 fraction. In general, a dye lifetime less than 1 ns is definitely preferable for our purposes. (ii) Decay of erythrosine B is dominated by a single lifetime with additional late-time power law contribution. Acridine orange exhibits two lifetimes arising from a two-state admixture, with the longer one dominating at times where a late-time power law behaviour would possibly emerge.
- For erythrosine B, a two-exponential fit was tested but performs definitely worse than the power-law one. Moreover, the two detectors measure incompatible values of τ_2 [22], making a two-state interpretation untenable. Indeed, the power-law coefficients β measured by both channels also differ, but this is consistent with basic QM and QFT expectations [10, 12].

7. Conclusions

In this paper, we have presented decay-intensity measurements of acridine orange, whose fluorescence is well described by the sum of two exponential components, consistently confirmed by both photon detectors. Although no late-time power-law behaviour has been observed, this study provides a valuable validation of our experimental setup for late-time decay measurements, as discussed in [22], and establishes the experimental conditions necessary for future searches of possible quantum-mechanical (and quantum-field-theoretical) deviations from the exponential decay law.

Acknowledgments

This work was supported by the Polish Minister of Science under the 'Regional Excellence Initiative' program (project RID/SP/0015/2024/01, sub-projects RID/2024/LIDER/08 and RID/2025/LIDER/02).

References

[1] L. Fonda, G.C. Ghirardi, A. Rimini, *Rep. Prog. Phys.* **41**, 587 (1978).

[2] B. Misra, E.C.G. Sudarshan, *J. Math. Phys.* **18**, 756 (1977).

[3] L.S. Schulman, *Phys. Rev. A* **57**, 1509 (1998).

[4] P. Facchi, S. Pascazio, *J. Phys. A* **41**, 493001 (2008).

[5] C. Balzer, T. Hannemann, D. Reiß, C. Wunderlich, W. Neuhauser, P.E. Toschek, *Opt. Commun.* **211**, 235 (2002).

[6] A.G. Kofman, G. Kurizki, *Nature* **405**, 546 (2000).

[7] L.A. Khalfin, *Doklady Akad. Nauk SSSR* **115**, 277 (1957).

[8] D.A. Dicus, W.W. Repko, R.F. Schwitters, T.M. Tinsley, *Phys. Rev. A* **65**, 032116 (2002).

[9] K. Urbanowski, *Phys. Rev. A* **50**, 2847 (1994).

[10] F. Giacosa, *Found. Phys.* **42**, 1262 (2012).

[11] F. Giacosa, G. Pagliara, *Mod. Phys. Lett. A* **26**, 2247 (2011).

[12] F. Giacosa, *Phys. Lett. B* **831**, 137200 (2022).

[13] P. Facchi, S. Pascazio, *Chaos Solitons Fractals* **12**, 2777 (2001).

[14] P. Facchi, S. Pascazio, *Phys. Lett. A* **241**, 139 (1998).

[15] F. Giacosa, K. Kyzioł, *Acta Phys. Pol. A* **146**, 704 (2024).

[16] S.R. Wilkinson, C.F. Bharucha, M.C. Fischer, K.W. Madison, P.R. Morrow, Q. Niu, B. Sundaram, M.G. Raizen, *Nature* **387**, 575 (1997).

[17] M.C. Fischer, B. Gutiérrez-Medina, M.G. Raizen, *Phys. Rev. Lett.* **87**, 040402 (2001).

[18] A. Crespi, F.V. Pepe, P. Facchi, F. Sciarrino, P. Mataloni, H. Nakazato, S. Pascazio, R. Osellame, *Phys. Rev. Lett.* **122**, 130401 (2019).

[19] S. Schael, ALEPH Collaboration, R. Barate, R. Brunelière et al., *Phys. Rept.* **421**, 191 (2005).

[20] C. Rothe, S.I. Hintschich, A.P. Monkman, *Phys. Rev. Lett.* **96**, 163601 (2006).

[21] J. Lakowicz, *Principles of Fluorescence Spectroscopy*, Vol. 1, Springer, 2006.

[22] F. Giacosa, A. Kolbus, K. Kyziol, M. Plodowska, M. Piotrowska, K. Szary, A. Vereijken, arXiv:2509.17163 (2025).

[23] T. Ban, K. Kasatani, M. Kawasaki, H. Sato, *Photochem. Photobiol.* **37**, 131 (1983).

[24] N. Miyoshi, K. Hara, I. Yokoyama, G. Tomita, M. Fukuda, *Photochem Photobiol.* **685** 8 (1988).

[25] S. Georghiou, *Photochem Photobiol.* **22**, 103 (1975).

[26] Y. Kubota, R.F. Steiner, *Biophysical Chemistry* **6**, 279 (1977).

[27] G. Cowan, *Statistical Data Analysis*, Oxford University Press, 2023.